

tion of heavy-atom parameters. Fig. 6 depicts the synthesis  $\rho_n(\mathbf{r})$  before and after the treatments (3)-(4) and (5)-(2).

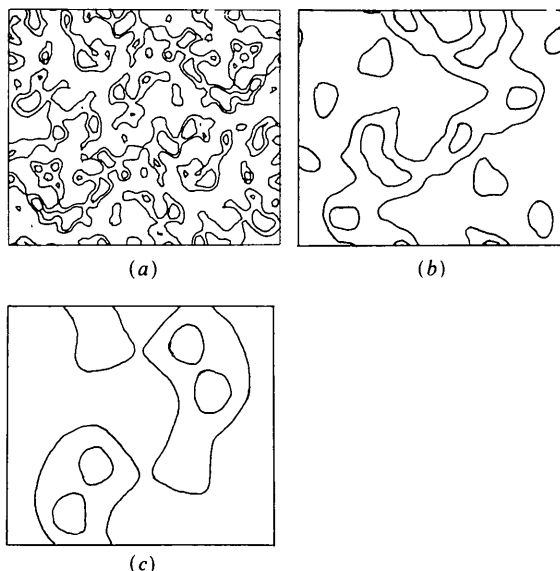


Fig. 6. Section  $z = 12/48$ : (a) the synthesis (11); (b) the synthesis (11) after treatment (3)-(4) ( $R = 10 \text{ \AA}$ ); (c) the synthesis (11) after treatment (5) and (2) ( $\rho_{\text{crit}}^{\text{max}} = 0.56$ ,  $\rho_{\text{crit}}^{\text{min}} = -0.047$ ,  $R = 10 \text{ \AA}$ ). Bounded is the region  $b(\mathbf{r}) > b^0$  which constitutes 40% of the cell volume.

*Acta Cryst.* (1989). **A45**, 39-42

## Polarization Anisotropy of Anomalous Scattering in Lithium Iodate and Effect of $K$ -Level Width

BY DAVID H. TEMPLETON AND LIESELOTTE K. TEMPLETON

*Department of Chemistry, University of California, Berkeley, CA 94720, USA*

(Received 23 March 1988; accepted 18 July 1988)

### Abstract

The anomalous scattering tensor, measured using synchrotron radiation with lithium iodate near the iodine  $K$  absorption edge, shows polarization anisotropy similar to that in the bromate ion, but lesser in magnitude: about 1 electron/atom at most. The reduction is explained by a greater natural width of the  $K$  level. Equally small or smaller anisotropy is predicted for any other absorption edge above 33 keV.

### 1. Introduction

X-ray dichroism occurs in some molecules near absorption edges as a result of transitions to electronic states which have symmetry that reflects the direc-

The authors thank O. M. Liginchenko for her help in preparing the manuscript.

### References

- BLUNDELL, T. L. & JOHNSON, L. N. (1976). *Protein Crystallography*. New York: Academic Press.
- BRICOGNE, G. (1976). *Acta Cryst.* **A32**, 823-847.
- CANNILLO, E., OBERTI, R. & UNGARETTI, L. (1983). *Acta Cryst.* **A39**, 68-74.
- HOPPE, W. & GASSMANN, J. (1968). *Acta Cryst.* **B24**, 97-107.
- LESLIE, A. G. V. (1987). *Acta Cryst.* **A43**, 134-136.
- NAMBA, K. & STUBBS, G. (1985). *Acta Cryst.* **A41**, 252-262.
- QURASHI, M. M. (1953). *Acta Cryst.* **6**, 103.
- SCHEVITZ, R. W., PODJARNY, A. D., ZWICK, M., HUGHES, J. J. & SIGLER, P. B. (1981). *Acta Cryst.* **A37**, 669-667.
- SHEVYREV, A. A. & SIMONOV, V. I. (1981). *Kristallografiya*, **26**, 36-41.
- SIMONOV, V. I. (1976). In *Crystallographic Computing Techniques*, edited by F. R. AHMED, K. HUML & B. SEDLÁČEK, pp. 138-143. Copenhagen: Munksgaard.
- URZHUMTSEV, A. G. (1985). *The Use of Local Averaging to Analyse Macromolecular Images in the Electron Density Maps*. Preprint, USSR Academy of Sciences, Pushchino.
- URZHUMTSEV, A. G., LUNIN, V. YU. & LUZYANINA, T. B. (1986). Tenth Eur. Crystallogr. Meet., Wrocław, Poland. Coll. Abstracts, pp. 51-52.
- VAINSHTEIN, B. K. & KHACHATURYAN, A. G. (1977). *Kristallografiya*, **22**, 706-710.
- WANG, B. C. (1985). *Methods Enzymol.* **115**, 90-112.
- ZWICK, M., BANTZ, D. & HUGHES, J. (1976). *Ultramicroscopy*, **1**, 275-277.

tional character of the chemical bonding. The anomalous scattering also depends on the direction of polarization of the radiation and needs to be represented by a tensor rather than a scalar function. Having found large effects of this kind for the pyramidal bromate ion near the  $K$  edge of bromine (Templeton & Templeton, 1985a) we were eager to test them in the iodate ion, which has analogous electronic structure and the same pyramidal shape. Lithium iodate, which crystallizes with two molecules per cell in the non-centrosymmetric space group  $P6_3$  (Rosenzweig & Morosin, 1966; de Boer, van Bolhuis, Olthof-Hazekamp & Vos, 1966), is a suitable material for observation of the dichroism because the threefold axes of all the iodate ions are parallel. This molecular orientation and the lack of a center of inversion permit

one to measure the complex scattering tensor by a diffraction technique used earlier for the tetrachloroplatinate ion (Templeton & Templeton, 1985*b*). Access to 33 keV radiation at the iodine *K* absorption edge was possible when a diffractometer (Nielsen, Lee & Coppens, 1986) was installed on a wiggler beam line at the Cornell High Energy Synchrotron Source (CHESS).

## 2. Method of the experiment

The components of the scattering tensor were determined as the variables in least-squares adjustments of observed and calculated structure-factor magnitudes, with the atomic coordinates and displacement parameters held constant. The values found by Svensson, Albertsson, Liminga, Kwick & Abrahams (1983) by neutron diffraction at 295 K were used. The atomic scattering tensors of all the iodine atoms can be represented by the matrix

$$\mathbf{f} = \begin{pmatrix} f_{\pi} & 0 & 0 \\ 0 & f_{\pi} & 0 \\ 0 & 0 & f_{\sigma} \end{pmatrix}$$

in a Cartesian coordinate system with *z* in the direction of the crystallographic *c* axis. For *s*-polarized radiation an azimuthal angle (the  $\pi$  setting) can be found for any Bragg plane such that the scattering factor reduces to  $f_{\pi} = f_0 + f'_{\pi} + if''_{\pi}$  (Templeton & Templeton, 1985*b*). For this  $\pi$  setting and *s* polarization the absorption of both incident and scattered beams corresponds to  $f''_{\pi}$ , and correction for absorption can be calculated in the usual manner. For *hk0* planes, *s* polarization, and azimuthal angle  $90^{\circ}$  from the  $\pi$  setting, the scattering factor is  $f_{\sigma} = f_0 + f'_{\sigma} + if''_{\sigma}$  and the absorption corresponds to  $f''_{\sigma}$ . A set of diffraction intensities measured at one of these kinds of azimuths can be used to derive  $f_{\pi}$  or  $f_{\sigma}$  as if  $\mathbf{f}$  were a scalar. For other settings, the calculated structure factor involves both principal values of the tensor, and dichroism complicates the absorption correction.

The determination of  $f''_{\sigma}$  in this way suffers because no Bijvoet differences exist among the *hk0* reflections, and the intensities are insensitive to the imaginary part of *f*. To improve the determination we included some *hkl* reflections in the measurements. For them the best setting is also  $90^{\circ}$  from the  $\pi$  setting, but the *c* axis cannot be made to coincide exactly with the *s* direction. Among those included in the calculations, the angular deviation ranged from  $5$  to  $17^{\circ}$ . At  $5^{\circ}$ , the scattering factor is 99%  $f_{\sigma}$  and 1%  $f_{\pi}$  and at  $15^{\circ}$ , 91%  $f_{\sigma}$  and 9%  $f_{\pi}$ . For this reason the anisotropy is underestimated by a small amount.

The imperfect polarization of the radiation affects the measurements of both  $f_{\pi}$  and  $f_{\sigma}$ . The observed intensities were divided by

$$P = 1 + 0.0638 \cos^2 2\theta$$

as a first-order correction for 88% polarization. This correction is valid for the scattering by lithium and oxygen and for the spherical average of the iodine tensor, but not for the anisotropy terms. Because the anisotropy is a small perturbation of the total scattering, we believe that the result of this approximation is to move  $f_{\pi}$  and  $f_{\sigma}$  toward each other by an amount that is a few percent of their difference.

## 3. Experimental

Crystals of  $\text{LiIO}_3$  were grown as follows: stoichiometric quantities of  $\text{Li}_2\text{CO}_3$  and  $\text{HIO}_3$  were dissolved in water, heated to 348 K, and cooled slowly. Then the water was allowed to evaporate at room temperature. A crystal with 17 faces and dimensions  $ca\ 0.20 \times 0.25 \times 0.27$  mm was used for the experiments.

Diffraction data were measured near the iodine *K* edge using a Huber diffractometer installed on the A2 station at CHESS. The wavelength was controlled by a monochromator with two reflections from Si(400), with a 1.0 cm carbon filter in front to reduce the heat load. It was calibrated according to the absorption edge observed in transmission through polycrystalline lithium iodate, assumed to be at  $0.37381 \text{ \AA} = 33.1665 \text{ keV}$  (Bearden, 1967). This calibration is in error by the amount of the chemical shift, if any, between iodate and elemental iodine. The degree of linear polarization of the beam, measured several times by horizontal and vertical scattering from a thin plastic sheet, was  $0.88 \pm 0.01$  with the beam limited vertically by a 1.5 mm slit 23 m from the source. Low counting rates prevented measurements on a finer scale.

Two lists of reflections and azimuthal angles were prepared. For 'perpendicular' experiments, the list included *h*  $-4$  to  $0$ , *k*  $-4$  to  $1$  and *l*  $3$  to  $10$  with  $\pi$ -setting azimuthal angles. It consisted of 279 reflections including repetitions of 004 (with  $\psi = 0^{\circ}$ ) measured every 13th or 15th time as a standard. The 'parallel' list contained 109 reflections chosen from the ranges *h*  $-8$  to  $0$ , *k*  $-8$  to  $0$ , and *l*  $-1$  to  $1$ , with  $\psi$  at  $90^{\circ}$  from the perpendicular setting, plus repetitions of  $\bar{6}00$  as a standard; 41 reflections were of the type *hk0*. A portion of each list, to the extent permitted by the vagaries of the synchrotron, was measured at each of several wavelengths. In a few cases repetitions were possible. The range of  $(\sin \theta)/\lambda$  was mostly  $0.105$  to  $1.196 \text{ \AA}^{-1}$  for the parallel sets and  $0.387$  to  $1.211 \text{ \AA}^{-1}$  for perpendicular ones.

Absorption corrections were made with our analytical absorption program ABSOR. Linear absorption coefficients were calculated by

$$\mu = (2Ne^2/mc^2)\lambda f'' = 83.4\lambda f'' \text{ cm}^{-1}$$

with  $\lambda$  in  $\text{\AA}$ . First  $f''$  and  $\mu$  were estimated from the absorption spectrum; then calculations were repeated

Table 1. Anomalous scattering of iodine, parallel polarization

keV	$f'_\sigma$	$f''_\sigma$	R (%)	N*
33·117	-6·7 (3)	1·4 (11)	2·7	96
33·162	-7·8 (2)	1·5 (7)	3·7	109
33·171	-8·6 (4)	3·9 (4)	3·1	76
33·173	-8·9 (2)	3·4 (4)	3·5	104
33·173	-8·5 (3)	4·0 (4)	3·1	105
33·174	-7·8 (4)	4·0 (4)	2·6	46
33·189	-6·9 (5)	4·2 (5)	3·3	52
33·209	-5·8 (4)	3·8 (8)	4·7	103
33·209	-6·2 (3)	3·7 (7)	4·0	105

\*Number of reflections

Table 2. Anomalous scattering of iodine, perpendicular polarization

keV	$f'_\pi$	$f''_\pi$	R (%)	N
33·120	-6·6 (2)	0·1 (7)	2·3	251
33·160	-8·5 (1)	0·9 (4)	2·2	201
33·169	-7·5 (4)	5·1 (5)	3·3	99
33·178	-7·9 (2)	5·1 (3)	3·2	244
33·186	-6·7 (2)	4·2 (4)	3·8	252
33·186	-6·6 (3)	4·2 (5)	3·2	215
33·188	-6·8 (2)	4·1 (3)	3·0	247
33·196	-5·8 (2)	2·9 (5)	2·0	60
33·207	-6·0 (2)	3·2 (3)	1·9	253

until the resulting  $f''$  was consistent with the  $\mu$  which had been used. Absorption correction factors ranged from 1·40 to 1·52 for the lowest  $\mu$  and from 8·28 to 13·36 for the highest one. Values for  $f'$  and  $f''$  are listed in Tables 1 and 2 and plotted in Fig. 1.

Polarized absorption spectra (Fig. 2) were measured by fluorescence technique with the crystal oriented so that the  $c$  axis was either parallel to or perpendicular to the  $s$ -polarization direction. The scintillation-counter detector of the diffractometer was detached and placed at one side of the incident beam. Obstruction by parts of the diffractometer prevented its placement at the ideal right-angle position.

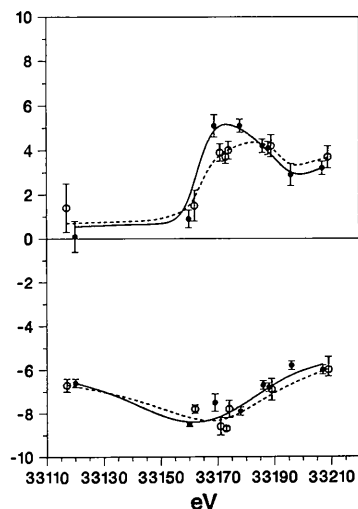


Fig. 1. Principal values of the anomalous scattering tensor: open circles,  $f'_\sigma$  (above) and  $f''_\sigma$  (below); solid circles,  $f'_\pi$  and  $f''_\pi$ .

#### 4. Discussion

As in bromate, the absorption edge for iodate is at lower energy and the edge resonance is stronger for perpendicular polarization than for parallel. The edge shifts, about 1 or 2 eV in each case, are similar, but the magnitude of anisotropy is less in iodate. The spectra in Fig. 2 show dichroism at the edge inflection region because of the difference in edge energy. In the region of maximum absorption, where bromate is most strongly dichroic, the iodate spectra show little difference; we attribute this to the sample thickness which exceeds the absorption length and limits the maximum signals. The greatest anisotropy of  $f''$  indicated by the diffraction experiments is about 1 in iodate compared with 6·6 in bromate, and the anisotropy of  $f'$  is even less. A small part of the reduction is caused by technical experimental details mentioned above. The rest is explained by a wider natural width of the  $K$  level: 10·6 eV in iodine, 2·52 eV in bromine (Krause & Oliver, 1979).

Anisotropy terms  $f'_2 = f'_\sigma - f'_\pi$  and  $f''_2 = f''_\sigma - f''_\pi$  for bromate are plotted in Fig. 3 (Templeton & Templeton, 1985a). The appearance of these curves, if the level width were like that in iodine, is estimated by convolution with a Lorentzian line shape:

$$f_r(E) = \frac{\Gamma}{2\pi} \int \frac{f(E') dE'}{(E' - E)^2 + (\Gamma/2)^2},$$

calculated with  $\Gamma = 10·6$  eV. The factor  $\Gamma/2\pi$  causes the areas under  $f_r$  and  $f$  to be equal. This transformation smears out most of the fine structure and reduces the maximum anisotropy of  $f''$  to 1·0, in agreement with the experimental result for iodate. The anisotropy of  $f'$  becomes less than 0·7 and is also consistent with the results for iodate.

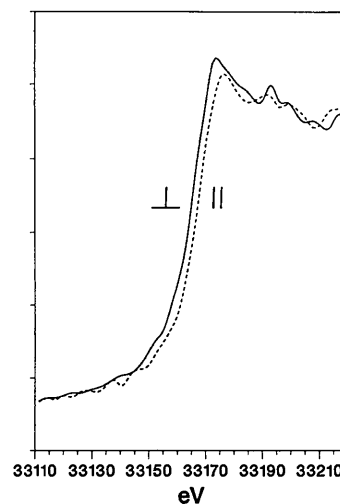


Fig. 2. Polarized absorption spectra for lithium iodate observed by fluorescence; sample thickness compresses the scale in the region of high absorption.

The  $K$ -level widths increase rapidly with atomic number beyond iodine, up to 96 eV for uranium. It seems unlikely that  $K$ -edge resonances for any of these heavy elements will be strong enough to compensate for the spreading of effects over wavelength any better than in the present case. No  $L$  absorption

edges occur in existing elements above 33 keV. Thus the high-energy region is not favorable for applications which would exploit this kind of dichroism or birefringence. Those who seek to avoid these complications may welcome this result. Another conclusion is that the search for examples of greatest anisotropy should be directed toward the long-wavelength region where levels are narrow.

We thank the staff members of CHESS whose cooperation and advice allowed us to complete this experiment with unfamiliar equipment in a single visit; we are particularly indebted to Finn Nielsen, Wilfried Schildkamp and Don Bilderback for assistance and to Philip Coppens and Boris Batterman for helpful discussions. This research was supported by the National Science Foundation under Grants CHE-8217443 and CHE-8515298. The measurements were made at CHESS which is supported by the National Science Foundation. Some facilities of the Lawrence Berkeley Laboratory, supported by the Director, Office of Energy Research, Office of Basic Energy Sciences, Chemical Sciences Division of the US Department of Energy under Contract No. DE-AC03-76SF00098 were used for analysis of the results.

#### References

- BEARDEN, J. A. (1967). *Rev. Mod. Phys.* **39**, 78-124.  
 BOER, J. L. DE, VAN BOLHUIS, F., OLTHOF-HAZEKAMP, R. & VOS, A. (1966). *Acta Cryst.* **21**, 841-843.  
 KRAUSE, M. O. & OLIVER, J. H. (1979). *J. Phys. Chem. Ref. Data*, **8**, 329-338.  
 NIELSEN, F. S., LEE, P. & COPPENS, P. (1986). *Acta Cryst.* **B42**, 359-364.  
 ROSENZWEIG, A. & MOROSIN, B. (1966). *Acta Cryst.* **20**, 758-761.  
 SVENSSON, C., ALBERTSSON, J., LIMINGA, R., KVICK, Å. & ABRAHAMS, S. C. (1983). *J. Chem. Phys.* **78**, 7343-7352.  
 TEMPLETON, D. H. & TEMPLETON, L. K. (1985a). *Acta Cryst.* **A41**, 133-142.  
 TEMPLETON, D. H. & TEMPLETON, L. K. (1985b). *Acta Cryst.* **A41**, 365-371.

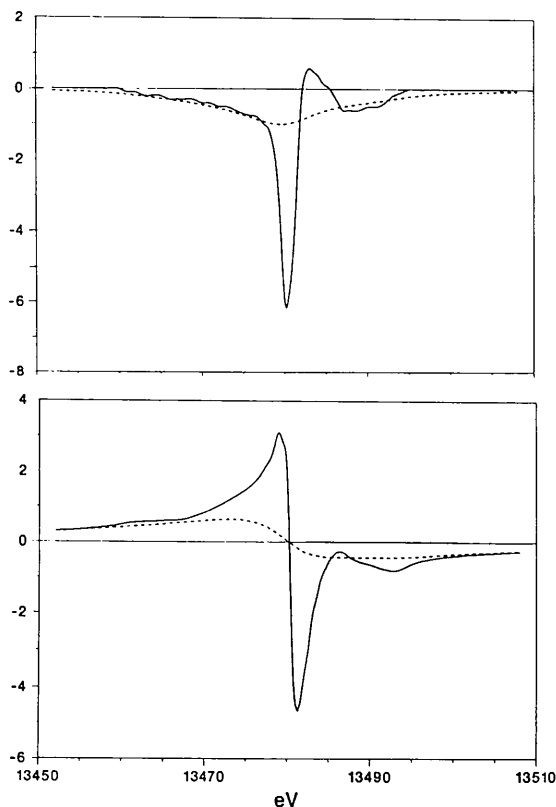


Fig. 3. Polarization anisotropy of anomalous scattering in sodium bromate,  $f''_{\sigma} - f''_{\pi}$  above,  $f'_{\sigma} - f'_{\pi}$  below. Solid curves show the actual values, broken curves the result of convolution with a line shape of 10.6 eV FWHM.

*Acta Cryst.* (1989). **A45**, 42-50

## A Memory-Efficient Fast Fourier Transformation Algorithm for Crystallographic Refinement on Supercomputers

BY AXEL T. BRÜNGER

*The Howard Hughes Medical Institute and  
 Department of Molecular Biophysics and Biochemistry, Yale University, New Haven, CT 06511, USA*

(Received 19 April 1988; accepted 20 July 1988)

### Abstract

A vectorizable algorithm for fast computation of structure factors and derivatives during refinement of macromolecular structures is presented. It is based

on fast Fourier transformations on subgrids that cover the unit cell of the crystal. The use of subgrids allows reduction of the total memory requirements for the computations without producing large overheads. The algorithm is applicable to all space groups. The